Electron capture and target ionization in collisions of bare projectile ions incident on helium

J. L. Shinpaugh,* J. M. Sanders, J. M. Hall,† D. H. Lee, H. Schmidt-Böcking,‡ T. N. Tipping, T. J. M. Zouros,§ and P. Richard

J.R. Macdonald Laboratory, Kansas State University, Manhattan, Kansas 66506

(Received 31 July 1991)

Absolute cross sections for the processes of single capture, transfer ionization, and single and double ionization were measured for C^{6+}, N^{7+}, O^{8+}, and F^{9+} projectiles incident on a helium target in the projectile velocity range of 0.25–2.0 MeV/amu. The cross sections were determined by measuring projectile-ion final charge states in coincidence with target recoil-ion final charge states. The single-capture and transfer-ionization cross sections were corrected for ionization from impurity charge states in the beam and for double-collision processes in the target gas cell. These corrections, which are necessary for the relative as well as the absolute cross sections, were found to be as large as 50% of the cross section. The measured cross sections are compared to the multistate, coupled-channel calculations of Shingal and Lin using an independent-electron model.

PACS number(s): 34.70.+e, 34.50.Fa

I. INTRODUCTION

In collisions of bare projectile ions with a helium target, five charge-changing processes are possible. These processes and their associated cross sections $\sigma_{qq'}^{kk'}$ may be defined as follows, where we use the notation k and k' to denote the initial and final charge states of the recoil ion, and q and q' to denote the initial and final states of the projectile: single ionization (SI), σ_{qq}^{01},

$$A^{q+}+\mathrm{He}\rightarrow A^{q+}+\mathrm{He}^{+}+e^{-} ;$$

double ionization (DI), σ_{qq}^{02},

$$A^{q+}+\mathrm{He}\rightarrow A^{q+}+\mathrm{He}^{2+}+2e^{-} ;$$

single capture (SC), σ_{qq-1}^{01},

$$A^{q+}+\mathrm{He}\rightarrow A^{(q-1)+}+\mathrm{He}^{+} ;$$

double capture (DC), σ_{qq-2}^{02},

$$A^{q+}+\mathrm{He}\rightarrow A^{(q-2)+}+\mathrm{He}^{2+} ;$$

and the process usually referred to as transfer ionization (TI), σ_{qq-1}^{02},

$$A^{q+}+\mathrm{He}\rightarrow A^{(q-1)+}+\mathrm{He}^{2+}+e^{-} .$$

The total one-electron transfer cross section is the sum of the single-capture and transfer-ionization cross sections, $\sigma_{qq-1}=\sigma_{qq-1}^{01}+\sigma_{qq-1}^{02}$.

For ion-atom collisions in general, single-electron processes are in many cases well understood quantitatively, while multielectron processes are less well understood and are often difficult to describe even qualitatively. Much attention has recently been given to the process of transfer ionization and its contribution to the total electron-capture mechanism in fast collisions [1–7]. While some of these studies have involved nonbare projectile ions, fully stripped projectile ions incident on a helium target provide the simplest multielectron collision systems and allow direct comparison with theory, without the problem of screening (or antiscreening) effects from projectile electrons. Although these effects may be minimal at higher projectile charges, they can be quite large at lower charges [8,9].

For collisions of bare projectile ions incident on helium in the intermediate- ($v\approx 2$ a.u.) to high- ($v>2$ a.u.) velocity regime, measurements of the relative contributions of single capture and transfer ionization to the total transfer process were first reported in 1979 by Horsdal Pedersen and Larsen [10] for proton projectiles in the energy range of 40 to 400 keV. These types of measurements were extended in 1984 by Shah and Gilbody [11] for H^+, He^{2+}, and Li^{3+} for approximately the same projectile-velocity range. Recently, measurements by Knudsen *et al.* [2] were made that extended the velocity range for H^+ and He^{2+} up to 1.0 and 1.5 MeV/amu, respectively. It is important in understanding total electron transfer that these types of measurements be extended to higher charged projectiles where TI can equal or exceed single capture. Only two such studies have been reported for bare-projectile-ion systems: one for 0.75- to 1.5-MeV/amu $O^{8+}+\mathrm{He}$ by Tanis *et al.* [3] and one for 0.37- to 2.0-MeV/amu $F^{9+}+\mathrm{He}$ by Shinpaugh *et al.* [5]. Nonbare projectile ions were also included in the study by Tanis *et al.*, and recently Datz *et al.* [6] have reported TI measurements for various charge states of iodine and uranium.

In the present work we report absolute cross-section measurements of single capture and transfer ionization that have been performed for projectile ions of 0.25- to 2.0-MeV/amu F^{9+}, 0.5- to 1.5-MeV/amu O^{8+}, and 0.5- and 1.0-MeV/amu C^{6+} and N^{7+} incident on a helium target. Cross sections for single and double ionization have also been determined. All of the cross sections are compared to the multistate, coupled-channel calculations of Shingal and Lin [12] using an independent-electron model (IEM).

II. EXPERIMENTAL ARRANGEMENTS

All measurements were performed at the J. R. Macdonald Laboratory at Kansas State University. The experimental apparatus has been described in detail previously [5,13] and shall only be briefly described here. Desired ion species were extracted from the EN tandem Van de Graaff accelerator, momentum analyzed, and the desired charge state directed to the collision region. As shown in Fig. 1, the beam was collimated by two sets of four-jaw slits separated by approximately 5 m and then passed through a "clean-up" magnet to deflect contaminant ions out of the beam. These contaminants consist of charge-state impurities from charge exchange of the beam with the slits and the residual gas in the beam line. The beam then passed through a differentially pumped gas cell, through a second magnet used to analyze the charge of the beam, and onto a position-sensitive detector. The pressure outside the gas cell between the clean-up magnet and the analyzing magnet was maintained at less than 10^{-7} Torr. The target gas was introduced into the gas cell, and the pressure controlled by an MKS Baratron system using a capacitance manometer. Target recoil ions produced from collisions with projectile ions were extracted by a static electric field and charge-state analyzed by their drift time through a time-of-flight spectrometer.

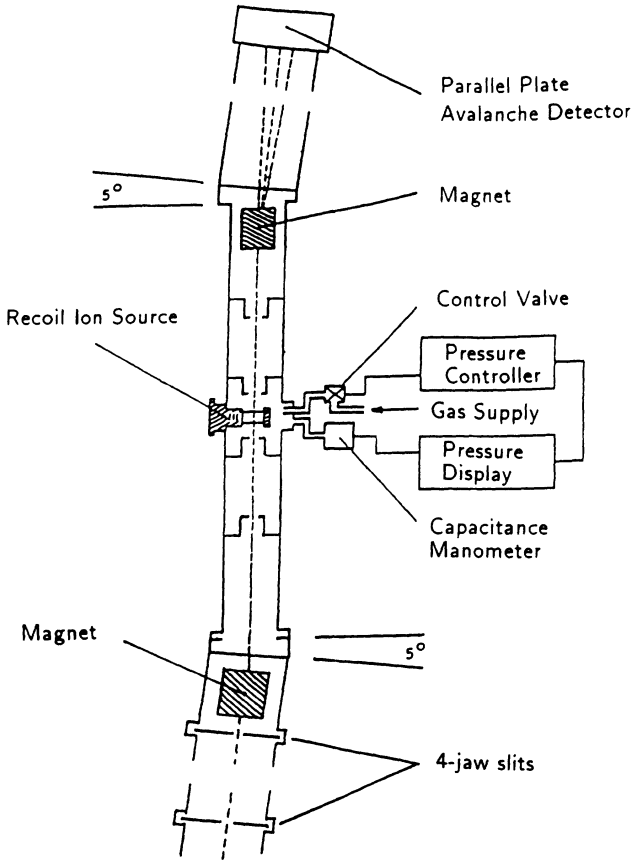

FIG. 1. Schematic diagram of the experimental apparatus.

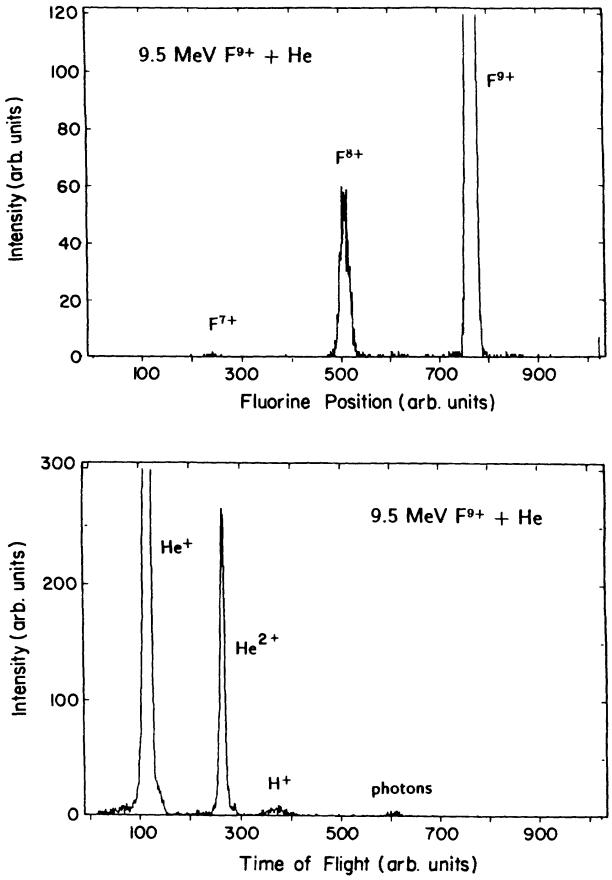

FIG. 2. Typical spectra for recoil-ion time of flight and projectile-ion position for 9.5-MeV F^{9+} incident on He.

Projectile-recoil coincidence yields were measured along with the projectile singles (all projectiles independent of recoils) in single-collision conditions (0.3- to 0.4-mTorr target-gas pressure) for bare projectile ions at the energies discussed above. Measurements were also performed for the hydrogenlike projectiles at each energy in order to determine ionization cross sections for these systems, which are needed in determining the SC and TI cross sections for the incident bare ions. Typical spectra for recoil-ion time of flight and projectile position are shown in Fig. 2 for the collision system of 9.5-MeV F^{9+} incident on He.

III. RESULTS

For the case of a bare F beam incident on He, the SI cross sections σ_{99}^{01} may be determined from the yield Y_{99}^{01} of F^{9+} ions coincident with He^{+} recoils by

$$\sigma_{99}^{01}=\frac{1}{n\epsilon}\frac{Y_{99}^{01}}{I_9}\ , \tag{1}$$

where I_9 is the incident F^{9+} projectile ion intensity, n is the areal target density, and ϵ is the recoil-ion detection efficiency. Similarly, the DI cross sections can be found by

$$\sigma_{99}^{02}=\frac{1}{n\epsilon}\frac{Y_{99}^{02}}{I_9} . \tag{2}$$

The expression used to determine the SC cross sections is given by

$$\sigma_{98}^{01}=\frac{1}{n\epsilon}\frac{Y_{98}^{01}}{I_9}-C_1^{SC}-C_2^{SC} , \tag{3}$$

where the correction terms C_1^{SC} and C_2^{SC} are

$$C_1^{SC}=\frac{1}{2}\frac{I_8^B}{I_9}(\sigma_{99}^{01}+\sigma_{88}^{01}) \tag{4}$$

and

$$C_2^{SC}=\frac{1}{2}\left[1-\frac{l}{L}\right]\frac{I_8-I_8^B}{I_9}(\sigma_{99}^{01}+\sigma_{88}^{01}) , \tag{5}$$

where I_8 is the total F^{8+} intensity, I_8^B is the number of contaminant F^{8+} ions in the beam (determined from background runs with no target gas in the cell), l is the length of the recoil-extraction region, and L is the total length of the gas cell.

The first correction term C_1^{SC} represents the contribution to the coincidence yield from single ionization of the target by contaminant ions in the projectile beam. This correction was found to be necessary because ionization cross sections can be several orders of magnitude larger than capture cross sections in this projectile-velocity range. Since the gas cell lies halfway between the cleanup magnet and the analyzing magnet, it may be assumed that half of the contaminant F^{8+} ions that reach the position-sensitive detector originate before the gas cell, and half after. Therefore, half of the He recoils associated with these contaminant ions come from ionization by F^{8+} ions, and half from ionization by F^{9+} ions which subsequently capture an electron to become F^{8+}. This correction increases with projectile velocity since capture decreases much more rapidly than ionization and was found to be as large as 50% of the single-capture cross section at 38 MeV for F^{9+} on He.

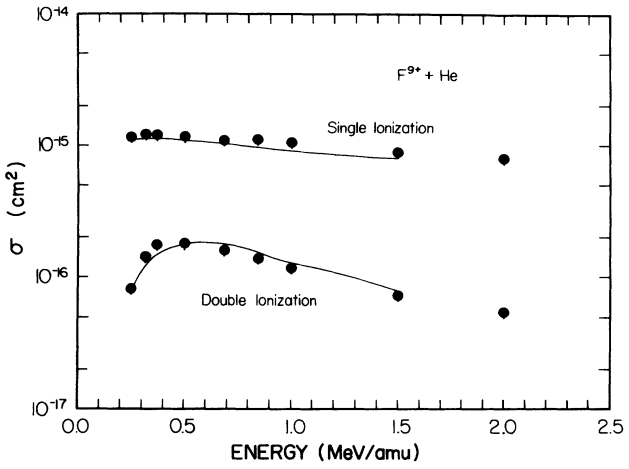

FIG. 4. Cross sections for single and double ionization for F^{9+} incident on He. The curves represent the calculations of Shingal and Lin [12].

The second correction term C_2^{SC} is necessary because the recoil detector views only part of the gas cell (about one-third), and it represents the contribution to the coincidence yield from double-collision processes where capture occurs in the gas cell, but not in the recoil-extraction region, and is accompanied by single ionization within the recoil-extraction region. This correction varies inversely with projectile velocity due to the dependence on charge transfer and was found to be as large as 14% of the single-capture cross section for 13-MeV F^{9+} incident on He at a target-gas pressure of 0.4 mTorr. The correction was reduced for lower energies by decreasing the He gas pressure in the cell to 0.3 mTorr.

Similar to single capture, the transfer ionization cross section may be found from

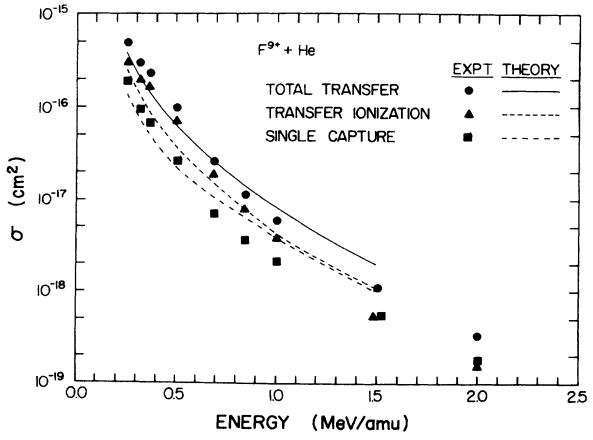

FIG. 3. Cross sections for total one-electron transfer, single capture, and transfer ionization for F^{9+} incident on He. The curves represent the calculations of Shingal and Lin [12].

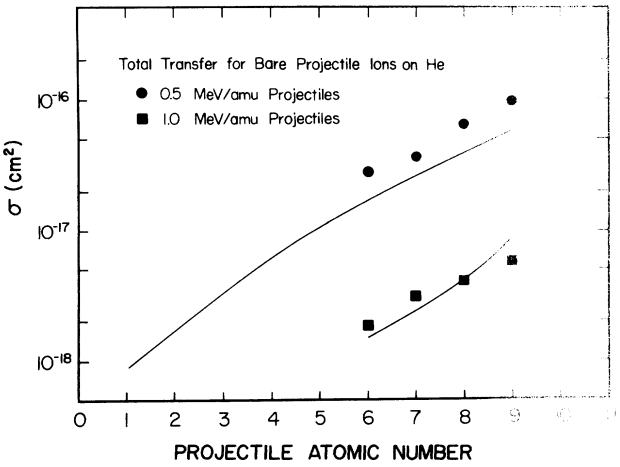

FIG. 5. Total one-electron transfer cross sections for 0.5- and 1.0-MeV/amu bare projectile ions incident on He. The curves represent the calculations of Shingal and Lin [12].

$$\sigma_{98}^{02}=\frac{1}{n\epsilon}\frac{Y_{98}^{02}}{I_9}-C_1^{\mathrm{TI}}-C_2^{\mathrm{TI}} \tag{6}$$

with

$$C_1^{\mathrm{TI}}=\frac{1}{2}\frac{I_8^B}{I_9}(\sigma_{99}^{02}+\sigma_{88}^{02}) \tag{7}$$

and

$$C_2^{\mathrm{TI}}=\frac{1}{2}\left[1+\frac{l}{L}\right]\frac{I_8-I_8^B}{I_9}(\sigma_{99}^{02}+\sigma_{88}^{02})\ . \tag{8}$$

The correction terms for TI are analogous to those for SC, as given in Eqs. (4) and (5), but involve double-ionization processes.

The recoil-ion detection efficiency ϵ in Eqs. (3) and (6) can be determined by comparing the coincidence yields with the total one-electron transfer cross sections. The sum of the single-capture and transfer-ionization partial cross sections must equal the total one-electron transfer cross section

$$\sigma_{98}=\sigma_{98}^{01}+\sigma_{98}^{02}\ , \tag{9}$$

so that

$$\sigma_{98}=\frac{1}{n\epsilon}\frac{Y_{98}^{01}}{I_9}-C_1^{\mathrm{SC}}-C_2^{\mathrm{SC}}+\frac{1}{n\epsilon}\frac{Y_{98}^{02}}{I_9}-C_1^{\mathrm{TI}}-C_2^{\mathrm{TI}}\ . \tag{10}$$

The efficiency is then

$$\epsilon=\frac{1}{n}\frac{Y_{98}^{01}+Y_{98}^{02}}{I_9}(\sigma_{98}+C_1^{\mathrm{SC}}+C_2^{\mathrm{SC}}+C_1^{\mathrm{TI}}+C_2^{\mathrm{TI}})^{-1}\ . \tag{11}$$

It should be noted, in the expression above, that the efficiency is implicitly contained in the correction terms within the ionization cross sections. Therefore, an iterative process was used to determine the efficiency. In the first stage, the ionization cross sections from the bare and the one-electron projectiles were assumed to be approximately equal, and the sum of these two cross sections (which is contained within the expression for each correction term) may be replaced by twice the bare-projectile ionization cross section. These cross sections can then in turn be replaced by their coincidence yields given in expressions (1) and (2). All of the terms on the right-hand side of Eq. (10) would then contain the factor $1/\epsilon$ explicitly, and Eq. (10) could be solved for ϵ. Thus, the efficiency ϵ could be expressed in terms of the coincidence yields and the total transfer cross section, all of which can be determined from a single coincidence measurement. This approximate efficiency was then used to calculate approximate ionization cross sections. In the second stage of the iterative process, these approximate ionization cross sections for the bare and one-electron projectiles were used in the correction terms in Eq. (11) to determine a final efficiency. In this fashion, the efficiency, correction terms, and cross sections could be determined. Any errors introduced by this process are thought to be negligible compared to the total experimental error.

Background spectra (no target gas admitted into the gas cell) were obtained before and after a spectrum was taken at each pressure in order to monitor the charge-state purity of the beam. A typical value for the amount of contaminants in the beam was one part in three thousand for a 1-MeV/amu F^{9+} beam. Most coincidence data were taken at a target-gas pressure of 0.4 mTorr to minimize collisions of He recoil ions with He atoms in the recoil-ion flight path, as well as to allow proper operating conditions for the microchannel plates (some of the low-energy data were taken at 0.3 mTorr to minimize double-collision events). Measurements were also performed using a gas jet instead of a gas cell to determine the effects of these He-He collisions. The results determined from the gas-jet and gas-cell experiments were in good agreement, so that it was deduced that neither of the charge states of helium was being preferentially lost over the other due to charge exchange (the presence of this process should also appear in the time-of-flight spectra as a tail on the He peaks).

In practice, the He partial cross sections in these coincidence experiments are difficult to measure because they are relatively small and the measurement is very sensitive to background fluctuations. Consequently, a high degree of scatter is observed in the data. Since the projectile-singles spectra are also measured in the coincidence experiments, the values of the absolute total transfer cross section from the coincidence and noncoincidence experiments can be compared. This can serve as a criterion for judging the merits of a particular run, and should allow for a more consistent set of data. If the total transfer cross section for a run was in good agreement with the "known" value (from the noncoincidence measurement), the ratio of transfer ionization to single capture was determined. To first order, this ratio is independent of the areal target density and the efficiency (although these factors do enter into the correction terms). The final value of this ratio is the weighted average determined from several (three to six) runs. The single-capture and transfer-ionization cross sections were then derived from this ratio R and the total transfer cross section:

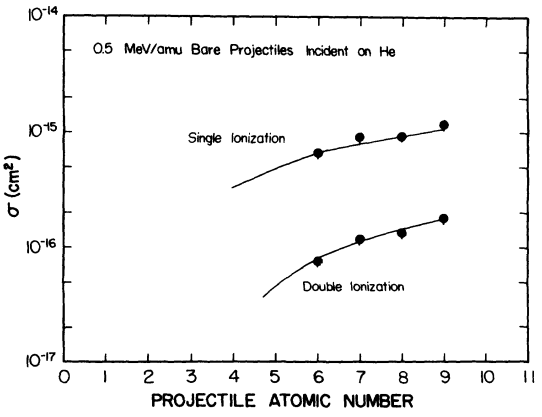

FIG. 6. Cross sections for single and double ionization for 0.5-MeV/amu bare projectile ions incident on He. The curves represent the calculations of Shingal and Lin [12].

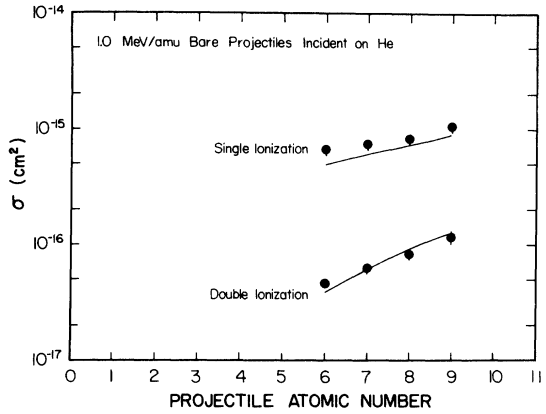

FIG. 7. Cross sections for single and double ionization for 1-MeV/amu bare projectile ions incident on He. The curves represent the calculations of Shingal and Lin [12].

$$\sigma_{98}^{01}=\frac{\sigma_{98}}{R+1}\ , \tag{12}$$

$$\sigma_{98}^{02}=\frac{R\sigma_{98}}{R+1}\ . \tag{13}$$

For F^{9+} ions incident on He, the measured cross sections for total one-electron transfer, single capture, and transfer ionization are shown in Fig. 3, along with the calculations of Shingal and Lin [12]. The single- and double-ionization cross sections are plotted in Fig. 4.

For 0.5- and 1.0-MeV/amu bare projectiles incident on He, the cross sections for total one-electron transfer are shown in Fig. 5. Single- and double-ionization cross sections as a function of atomic number are shown in Figs. 6 and 7 for 0.5- and 1.0-MeV/amu projectiles, respectively.

IV. DISCUSSION

The calculation method of Shingal and Lin [12] uses a coupled-channel semiclassical impact-parameter model employing a traveling atomic-orbital expansion to calculate single-electron processes (excitation, ionization, and capture) within the independent-electron model for an effective one-electron helium atom colliding with a bare ion. These single-electron processes are combined within the IEM to determine two-electron processes (transfer ionization, double capture, and double ionization). For determining the one-electron processes, an effective potential was used that gave the single-ionization energy of helium (0.9 a.u.). For the two-electron processes, however, an effective potential was used where the single-ionization energy of the electron was half of the double-ionization energy of helium (2.9 a.u.). This was done to account for a two-step mechanism where the first electron is removed and the second electron relaxes, becoming more tightly bound prior to removal. Both single- and double-ionization cross sections are described very

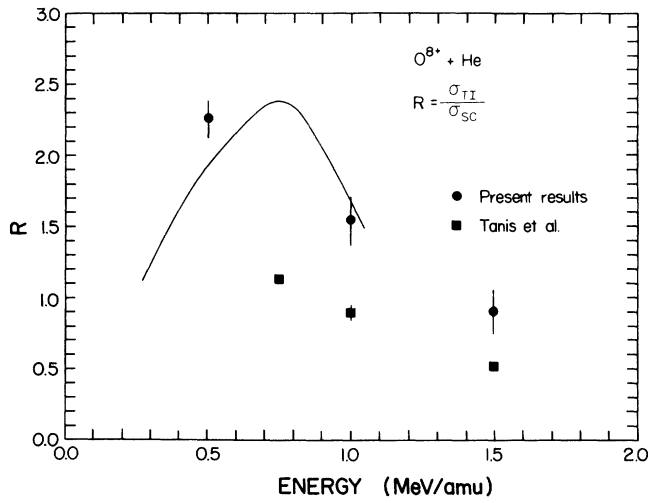

FIG. 9. The ratio of transfer ionization to single capture for O^{8+} incident on He. Included are the data of Tanis *et al.* [3]. The curve represents the calculations of Shingal and Lin [12].

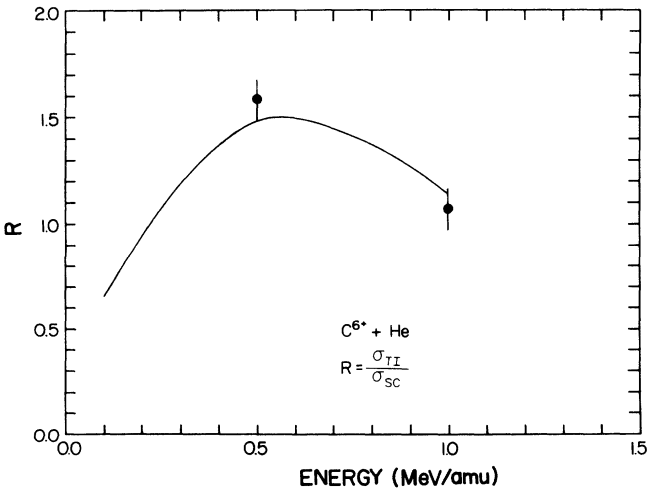

FIG. 8. The ratio of transfer ionization to single capture for C^{6+} incident on He. The curve represents the calculations of Shingal and Lin [12].

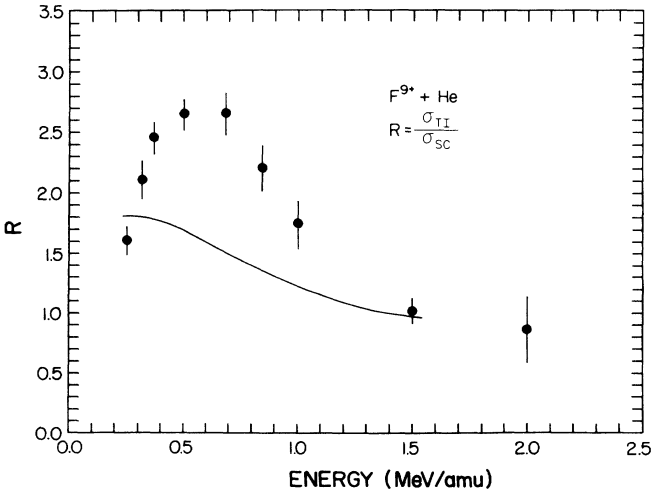

FIG. 10. The ratio of transfer ionization to single capture for F^{9+} incident on He. The curve represents the calculations of Shingal and Lin [12].

well within this method, as seen in Figs. 4, 6, and 7.

The calculated values of the total one-electron transfer cross sections for the 1.0-MeV/amu collision systems are in fair agreement with the data for $Z=6-9$, as seen from Fig. 5. The calculations for the 0.5-MeV/amu systems, however, tend to underestimate the measured values. This may be due to capture to higher n and l states that are not included in the calculation. This underestimation of the cross sections at low velocity, where capture to higher-n states occurs, can also be seen in the energy dependence of the F+He collisions in Fig. 3. If this is indeed the reason for the discrepancy at low energies, then the agreement should be enhanced by expanding the basis set in the calculations. Electron-correlation effects, which are not included in these calculations, may also play a role at these lower collision velocities. Datz *et al.* [6] have suggested that TI in highly charged ion-atom collisions in the intermediate-velocity range involves highly correlated double-capture of the electron pair, followed by electron loss to the continuum of the projectile.

The relative contribution of TI to the charge-transfer process may be observed more easily in the ratio R of transfer ionization to single capture. This ratio as a function of projectile velocity is shown in Figs. 8, 9, and 10 for C^{6+}, O^{8+}, and F^{9+} projectiles, respectively. As can be seen, the calculations appear to agree better with the lower charged projectiles. This again is probably due to the limited basis set employed in the calculation, since capture to higher-n states will occur with increasing projectile charge. The F^{9+} data show a maximum in the value of R similar to the structure that had been observed previously for the lighter projectiles He^{2+} and Li^{3+} [1,2,11]. The calculations for C^{6+} and O^{8+}, which are in good agreement with the present data, also show this behavior. Such a structure may reflect the transition to a lower-energy regime where double capture to doubly excited states followed by Auger emission is the predominant mechanism contributing to TI [3]. At higher energies ($\gtrsim 1$ MeV/amu), the direct (or two-step) mechanism, where one electron is captured and the other is ionized by impact ionization, should be dominant. Shake processes (final-state rearrangement) may also contribute to TI at high energies.

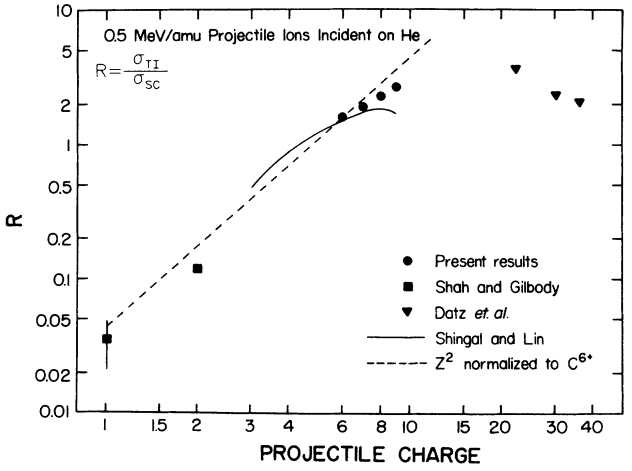

FIG. 11. The ratio of transfer ionization to single capture for 0.5-MeV/amu bare projectile ions incident on He. Included are the data of Shah and Gilbody [11] and Datz *et al.* [6]. The solid curve represents the calculations of Shingal and Lin [12] and the dashed curve represents a Z^2 scaling normalized to C^{6+}.

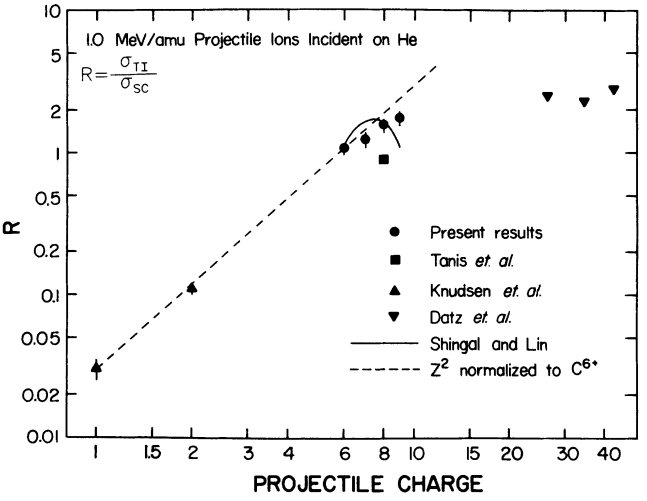

FIG. 12. The ratio of transfer ionization to single capture for 1.0-MeV/amu bare projectile ions incident on He. Included are the data of Tanis *et al.* [3], Knudsen *et al.* [2], and Datz *et al.* [6]. The solid curve represents the calculations of Shingal and Lin [12] and the dashed curve represents a Z^2 scaling normalized to C^{6+}.

The variation of R with projectile atomic number for the velocities of 0.5 and 1.0 MeV/amu is presented in Figs. 11 and 12. The dashed line in these figures represents a Z^2 scaling normalized to the C^{6+} value. For both velocity cases, the R values for low-Z projectiles agree well with this scaling, but R falls below this scaling for higher Z in the region of the present data. The data of Datz *et al.* [6] suggest that this ratio becomes constant or possibly decreases at higher-charge states.

V. CONCLUDING REMARKS

In summary, absolute cross sections for the processes of single and double ionization, single capture, and transfer ionization have been experimentally determined for collisions of bare projectile ions incident on helium. For the collision system of F^{9+} on He, these cross sections were determined for the projectile velocity range of 0.25 to 2.0 MeV/amu. These cross sections were also determined for C^{6+}, N^{7+}, and O^{8+} projectiles for the velocities of 0.5 and 1.0 MeV/amu. These cross sections were determined by measuring projectile-ion final charge states in coincidence with target recoil-ion final charge states. This was achieved by analyzing the recoil ions using time-of-flight spectroscopy and detecting the magnetically analyzed projectiles with a position-sensitive detector.

An important feature found in determining the cross sections for single capture and transfer ionization was the

necessity for two types of correction factors. The first type was produced from charge-state impurities present in the primary (bare ion) beam. The second type of correction originated from double-collision processes. These corrections were found to be necessary even in the determination of the relative cross sections, because the corrections to the single-capture cross sections are larger than those to the transfer-ionization cross sections. This has the effect of increasing the value of R, the ratio of transfer ionization to single capture, with respect to the uncorrected values. This may account for the discrepancy of the measured values of R reported here with those previously published by Tanis *et al.* for O^{8+} on He, which do not include these types of corrections [14].

It appears that the method of Shingal and Lin [12] gives a good description of single and double ionization, but single capture and transfer ionization remain a difficult calculation for highly charged projectiles. Further studies of the charge dependence of these processes would also be interesting, since the effects of projectile electrons are not well understood. Datz *et al.* [6] have reported values of TI and SC for 0.25-MeV/amu I^{9+} on He that give a value of R of approximately 0.8. This is half of the value reported here for the bare-ion case (F^{9+} + He, Fig. 10), so it would appear that projectile electrons can play a significant role in this region of projectile charge.

ACKNOWLEDGMENTS

This work was supported by the Division of Chemical Sciences, Office of Basic Energy Sciences, Office of Energy Research, U.S. Department of Energy.

*Present address: Institut für Kernphysik, Universität Frankfurt, Frankfurt am Main, Germany.

†Permanent address: Lawrence Livermore National Laboratory, Livermore, CA 94550.

‡Permanent address: Institut für Kernphysik, Universität Frankfurt, Frankfurt am Main, Germany.

§Permanent address: University of Crete and Research Center of Crete, Department of Physics, Heraklion, Greece.

[1] J. H. McGuire, E. Salzborn, and A. Müller, Phys. Rev. A **35**, 3265 (1987).

[2] H. Knudsen, D. H. Andersen, P. Hvelplund, J. Sørensen, and D. Ćirić, J. Phys. B **20**, L253 (1987).

[3] J. A. Tanis, M. W. Clark, R. Price, and R. E. Olson, Phys. Rev. A **36**, 1952 (1987).

[4] R. E. Olson, M. L. McKenzie, A. E. Wetmore, J. A. Tanis, M. W. Clark, and R. Price, Nucl. Instrum. Methods Phys. Res. B **27**, 590 (1987).

[5] J. L. Shinpaugh, J. M. Sanders, T. N. Tipping, D. H. Lee, T. J. M. Zouros, P. Richard, J. M. Hall, and H. Schmidt-Böcking, Nucl. Instrum. Methods Phys. Res. B **40/41**, 36 (1989).

[6] S. Datz, R. Hippler, L. H. Andersen, P. F. Dittner, H. Knudsen, H. F. Krause, P. D. Miller, P L. Pepmiller, T. Rosseel, R. Schuch, N. Stolterfoht, Y. Yamazaki, and C. R. Vane, Phys. Rev. A **41**, 3559 (1990).

[7] H. Damsgaard, H. K. Haugen, P. Hvelplund, and H. Knudsen, Phys. Rev. A **27**, 112 (1983).

[8] H. Knudsen, L. H. Andersen, P. Hvelplund, G. Astner, H. Cederquist, H. Danared, L. Liljeby, and K.-G. Rensfelt, J. Phys. B **17**, 3545 (1984).

[9] R. Hippler, S. Datz, P. D. Miller, P. L. Pepmiller, and P. F. Dittner, Phys. Rev. A **35**, 585 (1987).

[10] E. Horsdal Pedersen and L. Larsen, J. Phys. B **12**, 4085 (1979).

[11] M. B. Shah and H. B. Gilbody, J. Phys. B **18**, 899 (1985).

[12] R. Shingal and C. D. Lin, J. Phys. B **24**, 251 (1991).

[13] P. Richard, J. Hall, J. L. Shinpaugh, J. M. Sanders, T. N. Tipping, T. J. M. Zouros, D. H. Lee, and H. Schmidt-Böcking, Nucl. Instrum. Methods A **262**, 69 (1987).

[14] J. A. Tanis (private communication).